9th International Conference on Fracture Mechanics of Concrete and Concrete Structures
FraMCoS-9
V. Saouma, J. Bolander and E. Landis (Eds)
DOI 10.21012/FC9.184

IMPROVING FRACTURE TOUGHNESS OF POLYMER CONCRETE USING MWCNTS

ALA EDDIN M. DOUBA[*], MONEEB G. GENEDY [†], RAFI TAREFDER[**] AND MAHMOUD REDA TAHA [††]

[*]University of New Mexico
Albuquerque, NM USA
e-mail: Douba@unm.edu

[†] University of New Mexico
Albuquerque, NM USA
e-mail: moneeb@unm.edu

[*]University of New Mexico
Albuquerque, NM USA
e-mail: tarefder@unm.edu

[††] University of New Mexico
Albuquerque, NM USA
e-mail: mrtaha@unm.edu

Key words: MWCNTs, Fracture Toughness, Polymer Concrete, Tensile Strength

Abstract: Polymer concrete (PC) are used in bridge deck overlays due to its superior durability specifically freeze-thaw and corrosion resistance. The excellent durability of PC is related to its impermeable microstructure and good bond to concrete or steel substrates. However, there is an increasing need to improve PC resistance to crack propagation (fracture toughness) to enhance its fatigue resistance and extend its service life. Researchers showed that objective becomes possible using dispersed chopped synthetic fibers (6-12 mm long). However, this approach was criticized for its dramatic impact on PC flowability. Here we suggest improving fracture toughness of PC using Multi-Walled Carbon Nanotubes (MWCNTs).

PC mixes were produced using epoxy and standard aggregate with varying contents of MWCNTs being: 0 (Neat), 0.5, 1.0, 1.5 and 2.0 wt.% by weight of epoxy. Flowability of PC incorporating MWCNTs was tested. The tensile strength of PC incorporating MWCNTs was evaluated using direct tension test. A closed loop notched beam three-point bending test fracture test was used to evaluate fracture toughness of PC. The crack mouth opening displacement (CMOD) clip gage was used to provide feedback. The inverse analysis approach was used to extract the bilinear stress-crack opening displacement relation and calculate the fracture toughness (G_F) of PC with and without MWCNTs. It is shown that MWCNTs significantly improves the fracture toughness and toughness of PC without significantly impacting its flowability. Microstructural analysis using Fourier Transform Infrared Analysis (FTIR) of polymer used to produce PC explains the effect of incorporating MWCNTs.

1 INTRODUCTION

Polymer concrete (PC) is typically used in applications that require improved corrosion resistance, acid resistance, and high durability. PC is also commonly used in bridge deck overlays, manholes and has been recently suggested as a repair material for abandoned oil wells [1]. PC is produced by combining a polymer material (typically a thermoset polymer) with aggregate filler. Due to the nature of its applications, PC has high demand for high tensile strength, fatigue life and fracture toughness.

In the last decade, nanomaterials have been suggested as an alternative material to improve the mechanical and fracture characteristics of polymer composites [1-5]. Carbon nanotubes and specifically multi-walled carbon nanotubes (MWCNTs) have been the most common material used to improve fracture toughness of polymer composites. For instance, Yu et al. [3] showed that incorporating 3.0 wt.% MWCNTs as weight of polymer matrix, enabled a 33% increase in fracture toughness of carbon fiber composites [3]. Tang et al. reported 30% increase of fracture toughness (K_{1C}) compared with neat epoxy using 1.0 wt.% MWCNTs [4]. Tang et al. [7] showed an increase of fracture energy (G_F) by 56% using 1.0 wt.% ozone functionalized MWCNTs. Ganguli et al. [2] reported a much higher improvement in fracture toughness (K_{1C}) ranging between 40% and 80% when a limited content of 0.15 wt.% of ball-milled and acid-treated MWCNTs was incorporated in epoxy. Gojny et al. [9] showed only 6% improvement in fracture toughness when the content of amino-functionalised MWCNTs increased from 0.1 to 1.0 wt.%. The general agreement between researchers is incorporating MWCNTs results in improving fracture toughness of polymer composites. Nevertheless, a few issues remained questionable. First; what is the optimal content of MWCNTs to improve fracture toughness? Second; why a significant difference in these improvements are observed with the low and high content on MWCNTs? Third; what is the mechanism by which do MWCNTs change the fracture mechanics of polymer composite?. Some of those questions might be answered by considering the significance of MWCNTs dispersion on the performance of the polymer nanocomposite incorporating MWCNTs.

Nanomaterials are extensively small materials and possess relatively high surface area (100- 1000 m^2/g) [2]. This presents a challenge to properly disperse them within polymer matrix due to their tendency to agglomerate and clump. High shear mixing and ultra-sonication have been shown as necessary methods to improve dispersion of nanomaterials in polymers [6]. Surface functionalization of MWCNTs was shown as a method to improve dispersion of nanomaterials in polymer matrix. Obtaining a uniform dispersion of MWCNTs has been shown as an essential step to enable improvement in the polymer nanocomposite.

This paper investigates the significance of incorporating MWCNTs on the mechanical and fracture properties of epoxy PC. We examine the effect of incorporating 0.5, 1.0, 1.5 and 2.0 wt.% MWCNTs as weight of the epoxy resin on flowability, tensile strength, and fracture toughness of PC.

2 EXPERIMENTAL METHODS

2.1 Materials

Low modulus Polysulfide two-component siloxane epoxy polymer with silica powder filler was used to produce PC. The resin is mixture of Bisphenol A/Epichlorohydrin with silane while the hardener is Diethylenetriamine (DETA), Phenol, 4,4’-(1-methylethylidene)bis-, and Tetraethyllenepentamine. The powder filler is crystalline silica (quartz) and ceramic microspheres powder. MWCNTs of 20-30 nm outer-diameter, an inner dimension of 5-10 nm, and a length of 10-30 μm with no functional groups were used.

2.2 PC preparation

Dispersion of MWCNTs was performed using shear mixing and ultra-sonication. MWCNTs were added to the epoxy resin as percentage of weight of epoxy resin at different contents and heated to 110℃. The resin was

then mechanically stirred using magnetic stirrer under 800 rpm for two hours. This technique decreases the viscosity of the epoxy while producing significant shear forces to disperse the nanotubes. The epoxy resin was then dropped in ultra-sonication bath and degassed for two hours. The epoxy resin was left to cool down to room temperature for several hours.

To produce PC slurry, the epoxy resin (neat or with dispersed MWCNTs) and the epoxy hardener were added together in a 2:1 volume ratio as recommended by the manufacturer and mixed for 3 minutes at low speed. The aggregate filler was then added gradually to avoid entrapping air in the mix and the PC was mixed for 3 minutes to produce uniform slurry. Table 1 summarizes the PC mix proportions. PC specimens were then cast in two layers each compacted 25 times. Five specimens were cast for tension and fracture tests. Figure 1 shows the process of preparing MWCNTs-epoxy nanocomposite.

Table 1: Mix proportions for PC.

Designation	Resin (kg/m^3)	Hardener (kg/m^3)	Filler (kg/m^3)	MWCNTs content (kg/m^3)
PC-Neat	288	125	1560	0.00
PCNC-0.5				1.44
PCNC-1.0				2.88
PCNC-1.5				4.32
PCNC-2.0				5.76

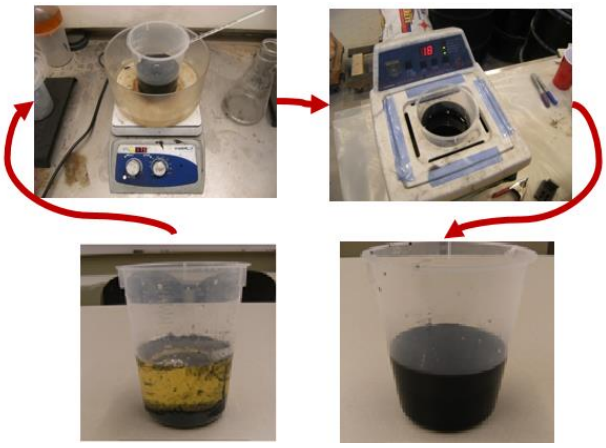

Figure 1: Steps for producing MWCNTs-epoxy nanocomposite for producing PC.

2.3 Flowability test

Flowability of the produced PC was measured using ASTM C1437 using a 70/100 mm with 50 mm height cone [10]. PC mixes were filled immediately after mixing with two layers each compacted 20 times. The flow table was then stroke 25 times spreading the PC uniformly. Four diameter reading with specific caliber were then added together to report the flowability reading of the specific mix. Figure 2 shows the process of flowability test of PC.

Figure 2: Flowability test of PC steps.

2.4 Tension test

ASTM D638 was used to perform tensile strength test of PC [11]. Type III specimen were produced using manufactured molds by the author complying with the standard per thickness ≈ 10 mm. The test was performed using MTS Bionix with 6.35 – 12.7 mm grips and an MTS Extensometer with 0.0001 resolution attached on the middle of each specimen for strain measurement as shown in Figure 3. The tension specimens were loaded in displacement control using 3.75 mm/min load rate. The displacement, strain and tension load to failure were measured.

Figure 3: Tension test of PC incorporating MWCNTs.

The toughness of PC mixes was estimated by calculating the area under the curve of the tensile stress-strain of PC up to failure using Equation (1) where U is the toughness, σ is the stress and ε is the strain of PC.

$$U=\sum_{i,j}\sigma_{ij}\,\Delta\varepsilon_{ij} \quad (1)$$

2.5 Fracture test

Three-point bending test setup of a notched beam was used to perform fracture test. The crack mouth opening displacement (CMOD) was recorded using specific clip gage. The test setup followed ACI 446 report on guidelines fracture toughness testing of concrete [12]. 150 mm length by 25 mm width and depth PC notched beams were casted and notched at 75 mm with 8.25 mm ± 5% depth and a thickness of 0.75 mm. The cantilever part of the specimen resulted in zero moment at the crack location when loaded with 75 mm span. A reference frame was manufactured in order to attach two Linear Variable Differential Transformers (LVDT) and correctly capture the displacement of the specimen under bending at the crack tip. Two knife edge plates were attached around the crack of 0.8 mm thickness to attach the CMOD and reference the LVDT. Figure 4 shows the test setup.

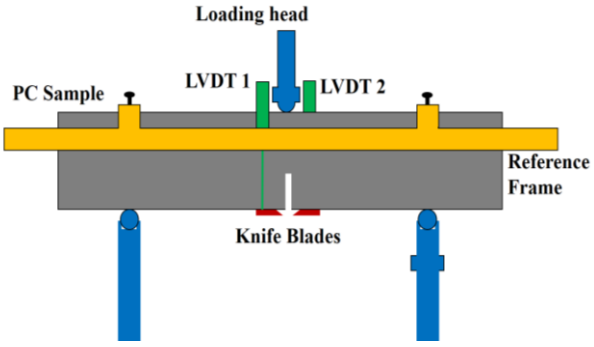

Figure 4: Fracture test setup.

Loading rate was determined to insure reaching peak load in 3-5 mins such that concrete softening effect to failure can be observed within 20-30 mins. Five specimens were tested per PC mix. Bi-linear curves were back-solved for using the method prescribed by ACI 446 report [12] and the fracture energy G_F was calculated using equation (13). Equations 2-13 summarizes the equations prescribed in ACI 446 report necessary for the calculation of fracture energy G_F. Equations 2 through 5 aim to determine an equivalent load due to self-weight and estimate the net plastic flexural strength. Using these values, the load-CMOD curves are corrected using least squares fitting prescribed in equations 6, 7 and 8. The results of the corrected curves are then used to resolve the plastic flexural strength and calculate the brittleness length as presented in equations 9 and 10. The area under the curve (representing the work of fracture W_F) is then calculated in equation 11. The CMOD axis intercept with slope of the initial softening curve is calculated in equation 12. The fracture energy for the specific specimen is calculated using equation 13.

$$P_0=mg\left(1-\frac{L}{2S}\right) \quad (2)$$

$$f_p=\frac{P_{max}S}{2Bb^2} \quad (3)$$

$$C_i=\frac{\Delta(CMOD)}{\Delta P'} \quad (4)$$

$$E=\frac{6Sa_0}{C_iBD^2}V_1(\alpha_0') \quad (5)$$

where, $\alpha_0=\frac{a_0+h}{D+h}$ and

$$V_1(\alpha)=0.8-1.7\alpha+2.4\alpha^2+\frac{0.66}{(1-\alpha)^2}+\frac{4D}{S}(-0.04-0.58\alpha+1.47\alpha^2-2.04\alpha^3)$$

$$X=\left(\frac{4D}{S}\right)^2\left(\frac{1}{(w_M-w_{MA})^2}-\frac{1}{(w_{MR}-w_{MA})^2}\right) \quad (6)$$

$$P_1=X(A+KX) \quad (7)$$

$$P_{1max}=P'_{max}+P_0 \quad (8)$$

$$f_{p1}=\frac{P_{1max}S}{2Bb^2} \quad (9)$$

$$l_1=\kappa D\left[\frac{11.2}{(x^2-1)^2}+\frac{2.365}{x^2}\right] \quad (10)$$

$$W_F=W_{Fm}+\frac{2A}{\delta_R+\delta_A} \quad (11)$$

$$w_1=1000\frac{2f_t}{E}\,l_1 \quad (12)$$

$$G_F=1000\frac{W_F}{Bb} \quad (13)$$

Notation

a_0 - Notch length (initial crack length)
A – Far-tail constant
b - Ligament length = D - a_0
B - Thickness of specimen
C_i - Initial compliance of beam specimen
CMOD - crack mouth opening displacement
D - Depth of specimen
E - Elastic modulus
f_t - Tensile strength
f_p - Net plastic flexural strength
g - Specific gravity = 9.81 m/s^2
G_F - mean fracture energy.
h - Distance from the CMOD measuring line to the specimen surface
K - Tail fitting parameter
l_1 - Brittleness length
L - Length of specimen
m - Mass of the specimen
N - Notch width
P - Total load on specimen
P_0 - Self-weight equivalent load
P' - Measured load on specimen
P_1 - Corrected load on specimen
P'_{max} - Effective peak load on a specimen
r - Distance from the measuring line of the displacement extensometers to the center plane of the specimen
S – Span of the test specimen
w_1 - Horizontal intercept of the linear initial portion of the softening curve
w_{MA} - CMOD at zero P_1
w_{MR} - CMOD at the end of the test
W_F - total work of fracture
X - Auxiliary variable for far tail fitting
α_0 - Relative notch length = a0/D
δ_A - Load point displacement at zero P_1
δ_R - Load point displacement at the end of test
κ – $1-\alpha_0^{1.7}$

It should be noted that the modulus of rupture was used for estimating f_t in the previous equations. Equation 14 was used to check the applicability of Linear Elastic Fracture Mechanics (LEFM). In equation 14, *l* is the specimen's least dimension, K_{1C} is the critical stress intensity factor, *E* is the elastic modulus and σ_y is the yield strength taken as the tensile strength of PC. The modulus of elasticity was determined with reference to stress-strain curves from the tension test.

$$l \geq 2.5\left(\frac{K_{1C}}{\sigma_y}\right)^2=2.5\left(\frac{\sqrt{G_F E}}{\sigma_y}\right)^2 \quad (14)$$

2.6 Microstructural analysis

Fourier Transform Infrared Spectroscopy (FTIR) was used to investigate the microstructure and explain the behavior of PC. Epoxy specimens of 25.4 cm^2 and 2 mm thickness were prepared with and without MWCNTs. The specimen was produced using similar mixes to that presented in Table 1 without filler to investigate the significance of MWCNTs on the chemical reaction of epoxy. 4000 scans were collected at a resolution of 4 cm^{-1} using a horizontal Attenuated Total Reflectance (ATR) and a DiComp Crystal. The DiComp crystal consist of a diamond ATR alongside Zinc Selenide focusing element. Scans of the FTIR were analyzed using PerkinElmer FTIR with Universal ATR accessory which were converted to absorbance using Kramers-Kronig equations [13].

3 RESULTS AND DISCUSSION

3.1 Flowability

Flowability test results are shown in Figure 5. Flowability test results of PC showed no significant decrease in PC flowability up to 1.0 wt.% MWCNTs content when compared with neat PC. At MWCNTs of 1.5 and 2.0 wt.%, PC showed a decrease of flowability of 17 and 26% respectively. Despite this decrease, PC incorporating 2.0 wt.% MWCNTs was still flowable and was possible to use to produce PC specimens. Our investigation showed that increasing the MWCNT's content beyond 2.0

wt.% will produce unflowable PC that would trap excess amount of air would not produce good PC.

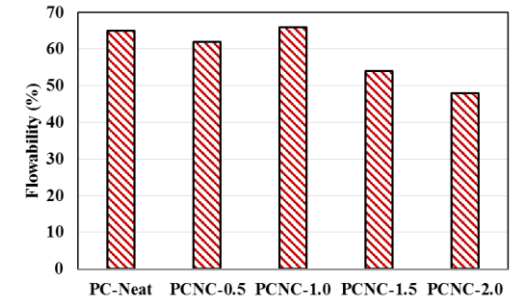

Figure 5: Flowability test results.

3.2 Tension test

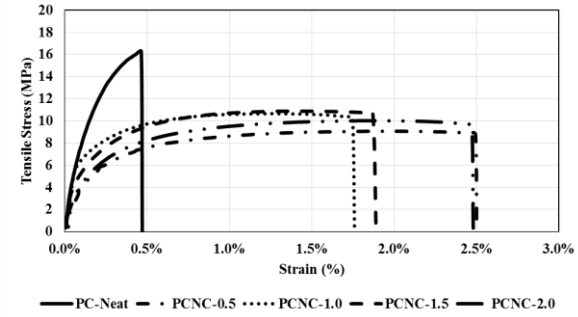

Figure 6: Stress-strain in tension test.

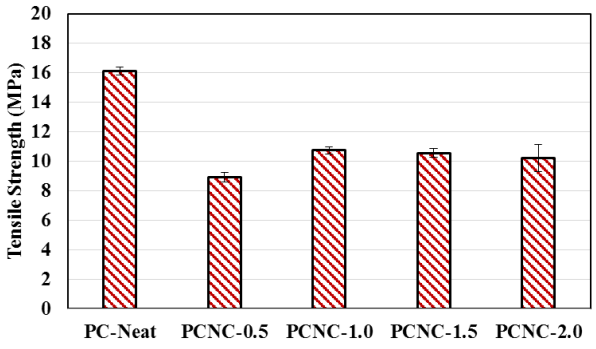

Figure 7: Tensile strength.

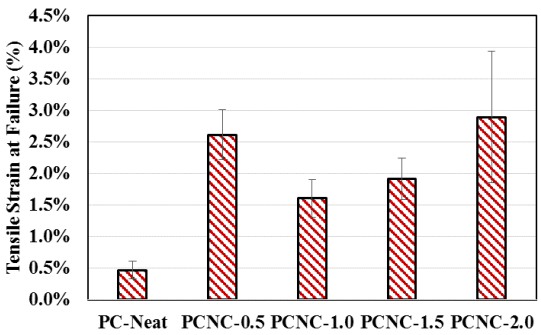

Figure 8: Tensile strain at failure in tension test.

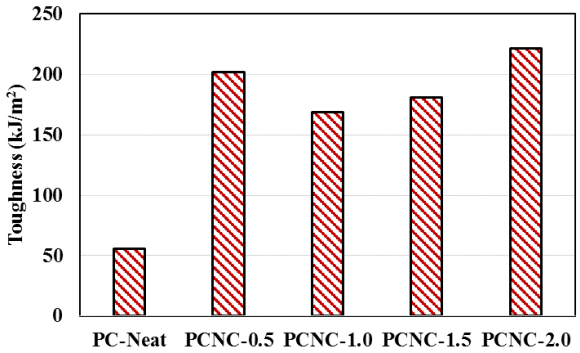

Figure 9: Toughness of PC in tension.

Results of the tension test showed that the stress-strain curves of PC incorporating MWCNTs were altered significantly. All PC incorporating MWCNTs showed lower strength and much higher strain at failure as shown in Figure 6. PCNC-2.0 and PCNC-0.5 reached a significant 2.5% strain at failure proving a high strength high strain material with a failure strain about one order of magnitude of strain at failure of normal concrete. The stress-strain diagrams were used to calculate the tensile strength, the strain at failure, and PC toughness using Equation (1).

Figure 7 shows the decrease of tensile strength with the incorporation of MWCNTs. The decrease was in the range of 33 to 45% with the largest decrease being that of PC with 0.5 wt.% MWCNTs. Increasing the content of MWCNTs beyond 1.0 wt.% showed no significant influence on the tensile strength of PC. This observation is in contrast to results reported early by others on the effect of functionalized MWCNTs which was reported to improve the tensile strength of latex modified concrete [14].

On the other hand, incorporating MWCNTs resulted in significant improve in strain at failure when compared with neat PC. The improvement in strain ranged between 242% and 516% as shown in Figure 8. Results of incorporating 1.0, 1.5 and 2.0 wt.% MWCNTs shows a linear trend of significant increase of strain at failure with the increase in content of MWCNTs. PCNC-0.5 demonstrated a different trend. At 0.5 wt.% content (for this specific epoxy matrix) MWCNTs seem to produce a nano-scale effect that is different than that

observed at a higher content. We believe that the amount of 0.5 wt. % might be the borderline separating between the MWCNTs acting as a nanocomposite and MWCNTs acting as a reinforcing fibers.

Using higher contents, MWCNTs exhibit reinforcing mechanism increasing the plastic strain without improving the tensile strength. The increase of strain at failure is associated with a significant increase in toughness (energy absorption to failure). Figure 9 shows similar general increase of toughness of PC with MWCNTs compared with neat PC by PC incorporating 2.0 wt. % MWCNTs having the highest increase in toughness of 295% compared with neat PC.

3.3 Fracture test results

The load-CMOD measurements of PC incorporating MWCNTs are shown in Figure 10. It is apparent that incorporating MWCNTs improved the tension stiffening of PC represented by the descending part of the load-CMOD curve. It should be noted that unlike ordinary concrete (OC), the CMOD observed with PC samples is significantly larger reaching values up to 9 mm. Figure 11 shows the extent of crack opening versus stress bilinear relationship.

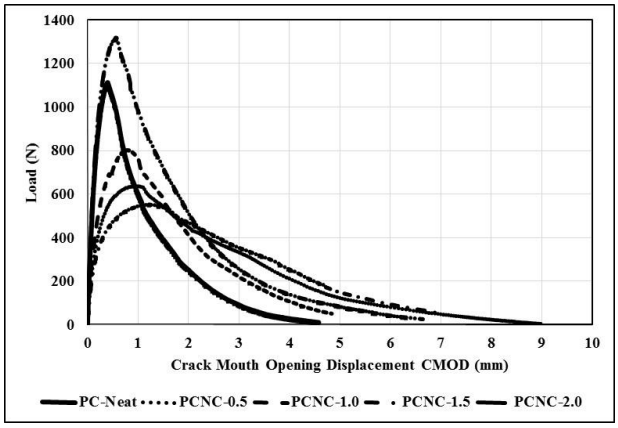

Figure10: Load-CMOD curves for PC incorporating MWCNTs.

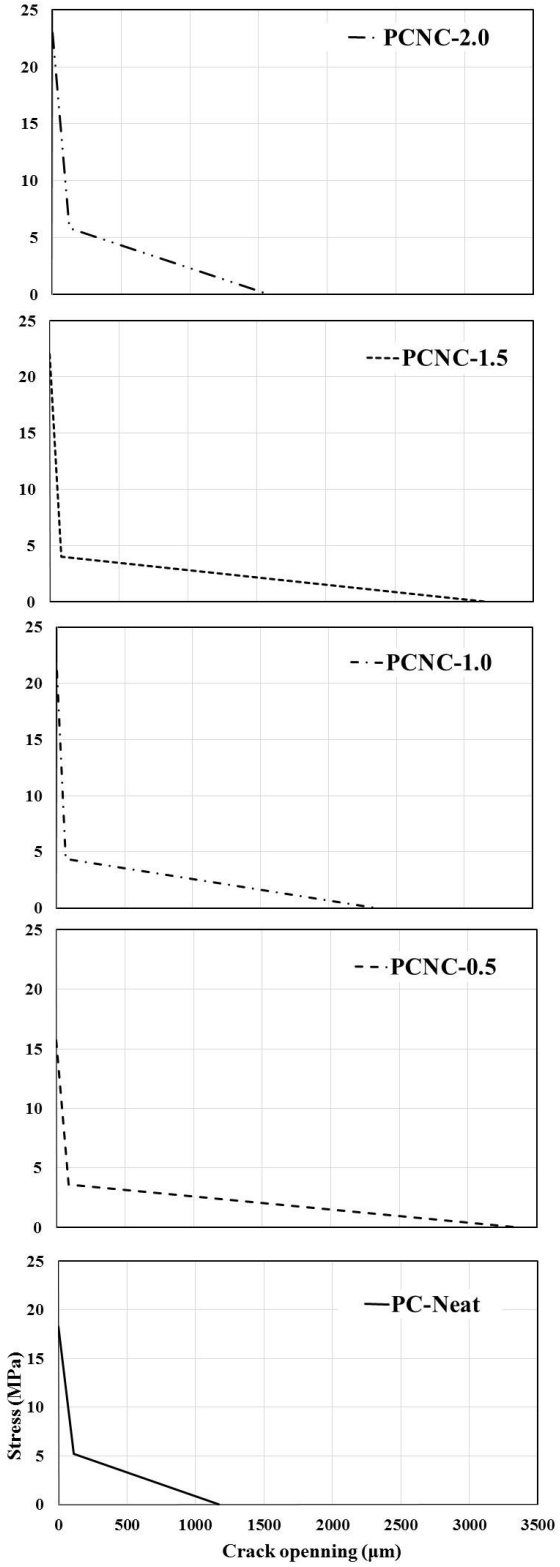

Figure11: Bi-linear approximation tension stiffening curves for PC incorporating MWCNTs.

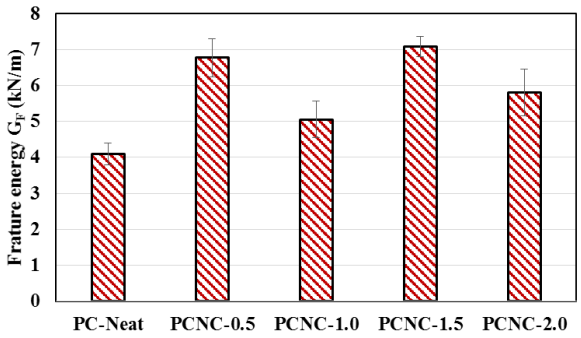

Figure 12: Fracture toughness energy.

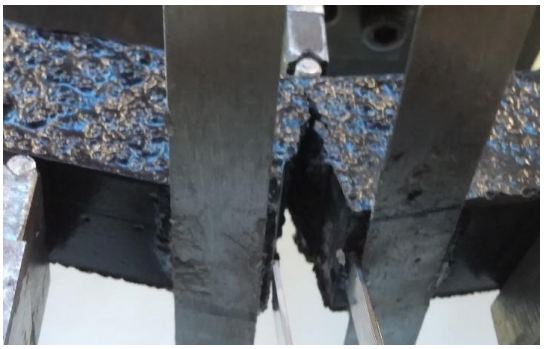

Figure13: CMOD for PCNC-2.0 at high CMOD.

It is important to note the significant improvement of the bilinear relationship with incorporating 0.5-1.5 wt.% MWCNTs. This improvement was lost by the increase in MWCNTs content to 2.0 wt.% The bilinear curve was used to calculate the fracture energy G_F that represent the fracture toughness of all PC mixes incorporating MWCNTs. The addition of MWCNTs resulted in increasing fracture toughness compared with neat PC in the range of 24% - 73%. PC incorporating 1.5% MWCNTs showed the highest increase in fracture toughness. At 1.0 wt.% MWCNTs, fracture toughness increased by 24% showing similar results to that of Yu et al. [3], Tang et al. [7] and Borowski et al. [15] observed due to incorporating MWCNTs in fibre reinforced polymer composites. PCNC-1.5 and PCNC-0.5 showed excessive CMOD to failure and a yield-like behavior in the curve softening region. Hence, reaching significant increase in fracture toughness by 66% and 73% respectively, compared with neat PC. Unlike the trend depicted in tensile test for toughness and strain, PCNC-2.0 showed a decrease in fracture toughness when compared to PCNC-1.5 and PCNC-1.0.

In fact, in fracture testing, PCNC-2.0 showed significant increase in stiffness attaining significantly high peak load which resulted in a decrease in its fracture toughness. The pattern of fracture toughness observations follows that from the tension test. At 0.5 wt.% content, MWCNTs act to improve the material through nano-scale effects on epoxy. At values higher than 0.5 wt.%, the significant increase in number of nanotubes present within the matrix, provides reinforcement that does not improve the strength but definitely helps in crack propagation resistance and thus improves fracture toughness of PC.

Equation 14 was used to ensure LEFM applies and to validate the results obtained. Table 3 shows the results of the critical limit of the least dimension for a material with the specified properties to be analyzed using LEFM. The least dimension required is 1490 mm and since all PC mixes have the same least dimension (25.4 mm).

Table 3: Least dimension check ensuring LEFM.

Value	PC-Neat	PCNC-0.5	PCNC-1.0	PCNC-1.5	PCNC-2.0
E (GPa)	14.2	6.07	11.2	9.37	5.53
G_F (kN/m)	4.09	6.77	5.06	7.08	5.80
σ_y (MPa)	16.1	8.9	10.7	10.6	10.2
l (mm)	560	1287	1231	1490	772

It is therefore obvious that LEFM does not apply to PC. This can be explained by the significant nonlinearity observed in PC behavior specifically when MWCNTs are included. Other fracture mechanics approaches such as quasi-brittle fracture mechanics (QBFM) shall be more appropriate to use [16]. Nevertheless, the above analysis show that significant improvement in fracture toughness of PC can be accomplished using MWCNTs.

3.4 Microstructural analysis

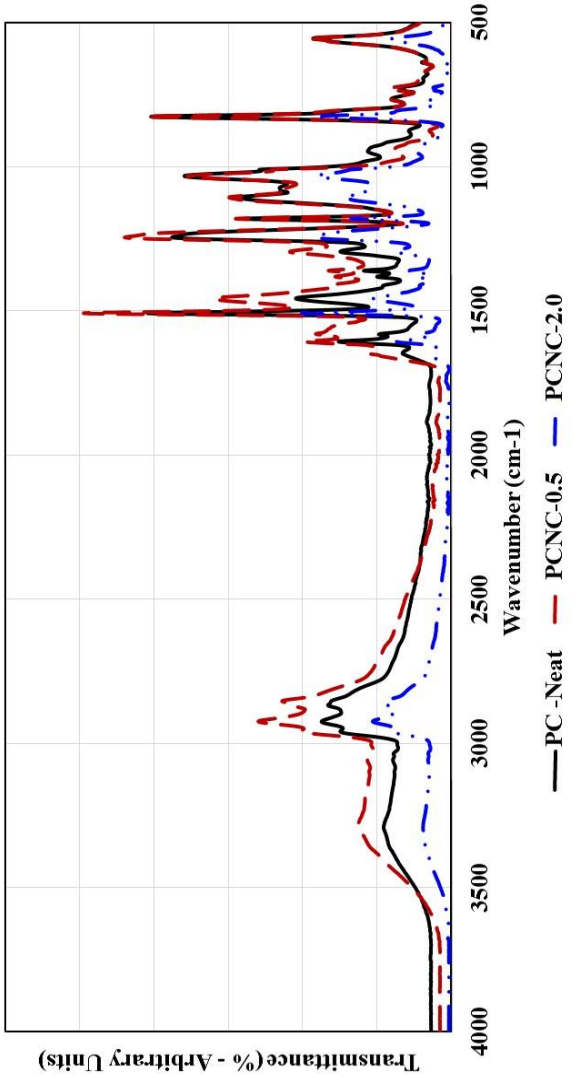

Figure 14: FTIR spectrographs of epoxy mixes including neat, 0.5 and 2.0 wt. % MWCNTs.

FTIR spectrographs of neat epoxy and epoxy with 0.5 and 2.0 wt. % of MWCNTs are shown in Figure 14. The characteristic peaks of the synthesized siloxane-epoxy/MWCNTs samples appeared at 3330–3500 cm^{-1} (O-H), 2750–2940 cm^{-1} (C-H), 1460 cm^{-1} (C-H, CH_2 and CH_3), 1039–1100 cm^{-1} (Si-O-Si and C-O-C), 1250–828 cm^{-1} (C-H in Si-CH_3), 560 cm^{-1} (Si-O-Si) [17-19]. A peak appears near 1605 cm^{-1} due to Si–C_6H_5 vibrations [20]. The remaining epoxy groups (oxirane ring) appeared at 940 cm^{-1}. The spectrographs of the three MWCNTs show no significant difference or shift and thus do not indicate any chemical interaction with MWCNTs because non-functionalized MWCNTs was used in the preparation of the PC composite. The ability of the relatively low content of non-functionalized MWCNTs (0.5 wt. %) to alter the mechanical properties might be attributed to the interaction between the nanoscale MWCNTs and epoxy. FTIR peaks in the spectrographs show that the peaks of the epoxy compounds in epoxy incorporating 0.5 wt. % MWCNTs are higher in magnitude than those of the neat epoxy. More interestingly, FTIR peaks of epoxy incorporating 2.0 wt.% MWCNTs are lower in magnitude than those of neat epoxy. The above observation can be explained by considering the ability of MWCNTs to hinder epoxy reaction. At a low MWCNTs content < 0.5 wt.%, it seems that MWCNTs inhibit epoxy reaction resulting in lower cross-linking than that of neat epoxy. The reduced cross-linking in its turn results in reducing PC strength and improving PC strain at failure and fracture toughness.

On the other hand, increasing the MWCNTs content gradually results in reducing MWCNTs effect on epoxy reaction. That might be explained by the fact that MWCNTs will tend to agglomerate at high content which would reduce their significance on the epoxy reaction. It is important to also note that high content of MWCNTs such as 2.0 wt.% might entrap air and thus reduce strength. However, the relatively large MWCNTs content helps in maintaining the integrity of PC and allows it to slightly improve the strength and strain at failure. It is apparent that the significance of MWCNTs on strength and fracture can be explained based on its chemical effect at relatively low content< 0.5 wt.% but the explanation becomes extremely complex with many interdependent factors at high MWCNTs contents. Further research is warranted to measure the cross-linking density of epoxy incorporating different MWCNTs contents.

4 CONCLUSIONS

The significance of incorporating MWCNTs in PC during PC fabrication was investigated. Flowability, tensile strength and fracture toughness of PC incorporating MWCNTs were investigated. Several PC mixes incorporating 0,

0.5, 1.0, 1.5 and 2.0 wt.% of MWCNTs were tested for flowability, tensile capacity, tensile strain, toughness, fracture toughness and through microstructural analysis using FTIR. The experimental results showed significant increase in tensile strain and toughness in the ranges of 242% - 516% and 201% to 295% respectively with increasing content of MWCNTs. However, a decrease in the tensile strength of in the range of 33% - 45% was also observed. Fracture tests showed also a significant increase in fracture toughness of PC incorporating MWCNTs in the range of 24% to 73% compared with neat PC.

There seems to be a threshold of MWCNTs content, beyond which the effect of MWCNTs changes from nano-effect to a fiber reinforcing effect. This threshold seems to be at or lower than 0.5 wt.%. At low contents, MWCNTs seem to have chemical effect by inhibiting epoxy reaction and reducing epoxy cross-linking. This results in the observed decrease in strength and significant increase in strain at failure. Further research is warranted to quantify the significance of MWCNTs on cross-linking of epoxy used in PC.

With increasing MWCNTs content, no further nano-effect takes place, but rather, MWCNTs act as microfibers. With increasing MWCNTs, the viscosity of polymer increases and thus the flowability of PC reduces making higher chance for entrapping air and reducing the overall strength. While this effect was pronounced in tension, little significance was observed when testing fracture toughness as the increased MWCNTs also enabled better crack arresting mechanism and thus improved fracture toughness of PC. The use of LEFM is not suitable to identify accurate estimate for fracture toughness of PC with MWCNTs. Nevertheless, the reported values provide insight on the significance of MWCNTs on strength and fracture of PC. Further work shall be done to quantify fracture toughness of PC using QBFM methods and to further link the change of mechanical characteristics of PC to changes in the epoxy matrix due to incorporating MWCNTs.

5 ACKNOWLEDGMENT

This work is funded by Southern Plains Transportation Center (SPTC). This support is greatly appreciated. The authors would like to extend their thanks to Transpo Industries Inc. for donating the polymer materials used in this research. The authors also extend their thanks to Ms. Amina Mannan for her help in conducting FTIR analysis and for Dr. Usama Kandil for his help in analysis of FTIR data.

REFERENCES

[1] M. Genedy, J. Stormont, E. Matteo and M. Reda Taha. Examining epoxy-based nanocomposites in wellbore seal repair for effective CO2 sequestration. *Energy Procedia*. 2014; 63, 3, 5798-5807.

[2] S. Ganguli, H. Aglan, P. Dennig & G. Irvin. Effect of loading and surface modification of MWCNTs on the fracture behavior of epoxy nanocomposites. *Journal of Reinforced Plastics and Composites*, 2006; 25(2), 175-188.

[3] N. Yu, Z. H. Zhang & S. Y. He. Fracture toughness and fatigue life of MWCNT/epoxy composites. *Materials Science & Engineering A*, 2008; 494(1-2), 380-384.

[4] L. C. Tang, Y. J. Wan, K. Peng, Y. B. Pei, L. B. Wu, L. M. Chen, .G. Q. Lai. Fracture toughness and electrical conductivity of epoxy composites filled with carbon nanotubes and spherical particles. *Composites Part A: Applied Science and Manufacturing*, 2013; 45(5453), 95-101.

[5] P. Thakre, D. Lagoudas, J. Riddick, T. Gates, S. J. Frankland, J. Ratcliffe, .E. Barrera. Investigation of the effect of ingle wall carbon nanotubes on interlaminar fracture toughness of woven carbon fiber--epoxy composites. *Journal of Composite Materials*, 2011; 45(10), 1091-1107.

[6] N. Grossiord, J. Loos, O. Regev, C. E. Koning. Toolbox for dispersing carbon nanotubes into polymers to get conductive nanocomposites. *Chemistry of Materials*, 2006; 18: 1089-1099.

[7] L. C. Tang, H. Zhang, J. H. Han, X. P. Wu & Z. Zhang. Fracture mechanisms of epoxy

filled with ozone functionalized multi-wall carbon nanotubes. *Composites Science and Technology*, 2011; 72(1):7–13.

[8] A. T. Seyhan, M. Tanoğlu &K. Schulte. Tensile mechanical behavior and fracture toughness of MWCNT and DWCNT modified vinyl-ester/polyester hybrid nanocomposites produced by 3-roll milling. Materials Science & Engineering: A, 2009; 523(1/2).

[9] F. H. Gojny, M. H, G, Wichmann, U. Köpke, B. Fiedler & K. Schulte. Carbon nanotube-reinforced epoxy-composites: enhanced stiffness and fracture toughness at low nanotube content. *Composites Science and Technology*, 2004; 64(15), 2363-2371.

[10] ASTM C1437-13. Standard test method for flow of hydraulic cement mortar. PA. 2013

[11] ASTM D638-14. Standard test method for tensile properties of plastics. PA. 2014

[12] ACI Committee 446, Report 5, Fracture Toughness Testing of Concrete. *American Concrete Institute*, 2009.

[13] P. Griffiths, J.A. de Hasseth, *Fourier Transform Infrared Spectrometry,* 2nd ed.; Wiley-Blackwell: Hoboken, NJ, USA, 2007.

[14] E. Soliman, U. F. Kandil, M. M. Reda Taha, M.M. The Significance of Carbon Nanotubes on Styrene Butadiene Rubber (SBR) and SBR Modified Mortar", *Materials and Structures*, 2012, 45 (6) 803–816.

[15] E., Borowski, E., Soliman, U. F. Kandil, M. M. Reda Taha, Interlaminar Fracture Toughness of CFRP Laminates Incorporating Multi-Walled Carbon Nanotubes, *Polymers*, 7 (6): 1020-1045, 2015.

[16] S. P. Shah, S. E. Swartz, C. Ouyang, *Fracture Mechanics of Concrete: Applications of Fracture Mechanics to Concrete, Rock and Other Quasi-Brittle Materials*, 1995, Wiley.

[17] L., Byczynski, M., Dutkiewicz, H., Maciejewski, Synthesis and properties of high-solids hybrid materials obtained from epoxy functional urethanes and siloxanes. *Progress in Organic Coatings*; 2015, 84, 59–69.

[18] S. Wang, Y. Li, X. Fei, M. Sun, C. Zhang, Y. Li, Q.o Yang, X. Hong; Preparation of a durable superhydrophobic membrane by electrospinning poly (vinylidene fluoride) (PVDF) mixed with epoxy–siloxane modified SiO2 nanoparticles: A possible route to superhydrophobic surfaces with low water sliding angle and high water contact angle; *Journal of Colloid and Interface Science*; 2011, 359 (2), 380–388.

[19] Y. Kwon, B. Yim, J. Kim, J. Kim; Mechanical and wetting properties of epoxy resins: Amine-containing epoxy-terminated siloxane oligomer with or without reductant, *Microelectronics Reliability*; 2011, 51 (4), 819–825.

[20] C. Hu, G. Xu, X. Shen, C. Shao, X. Yan; The epoxy-siloxane/Al composite coatings with low infrared emissivity for high temperature applications, Applied Surface Science; 2010, 256 (11), 3459–3463.